

# PREDICTING THE SHEAR CRACK LOCATION IN RC BEAMS WITH RANDOM CRACKS USING THE CRACK DENSITY PARAMETER

Ionut Ovidiu TOMA<sup>\*1</sup>, Tomohiro MIKI<sup>\*2</sup> and Junichiro NIWA<sup>\*3</sup>

## ABSTRACT

In this study, a procedure for determining the location of the shear crack in RC beams with randomly distributed cracks before loading is proposed. The method is based on the crack density parameter which is defined as the ratio between the area of the cracks and the area of concrete of a beam. The procedure is rather straight forward and shows good results for this type of damaged concrete specimens ranging from predicting the shear span where the failure is more likely to occur to a more accurate prediction of the shear crack location.

**Keywords:** random cracks, crack density, shear crack location

## 1. INTRODUCTION

The problem of how shear failure occurs in reinforced concrete beams, despite numerous extensive studies over the last 50 years [1], still remains unresolved. This type of failure, being a brittle one with sudden collapse of the concrete structural element, is to be avoided at all times. This is in strong contrast with the flexural failure. For typically under-reinforced concrete beams, flexural failure occurs by yielding of the longitudinal reinforcement accompanied with obvious cracking of concrete and large deflections that gives ample warning about the imminent failure of the specimen and provides the opportunity to take corrective measures.

The probability of brittle shear failure to occur in concrete elements that are already affected by deleterious agents (e.g. Alkali Silica Reaction) and exhibit distributed cracks is even higher. That is why it is important to know the shear carrying capacity of such members and, if possible, to know in which shear span the failure is more likely to occur.

The present study proposes a new and simple method to determine the location of the critical shear crack in concrete beams with distributed cracks. The procedure gave good results ranging from predicting the shear span where the failure is more likely to occur to a more accurate prediction of the shear crack location.

## 2. MATERIALS

### 2.1 Concrete

For this study a concrete with a design compressive strength of 30 N/mm<sup>2</sup>, obtained from uniaxial compression tests on cylinders (according to JIS A 1108), at 7 days, was considered. Five different mix proportions were used as summarized in Table 1. The strength of each concrete mix was measured at the day of testing.

### 2.2 Reinforcement

The longitudinal reinforcement used in this study is of the deformed PC bar type and its material specifications are according to JIS G 3109. The bars have a nominal diameter of 22 mm, with an area of  $A_{bar} = 387.1 \text{ mm}^2$ , an elastic modulus  $E = 2 \times 10^5 \text{ N/mm}^2$  and a yield strength  $f_y = 930 \text{ N/mm}^2$ .

### 2.3 Steel fibers

Steel short fibers used in this study are with crimped ends, similar to the ones used in previous studies [2]. The length is  $L_f = 30 \text{ mm}$  and the diameter is  $d_f = 0.6 \text{ mm}$ . The material properties are: tensile strength  $f_u = 1000 \text{ N/mm}^2$  and elastic modulus  $E = 2.1 \times 10^5 \text{ N/mm}^2$ .

### 2.4 Expansion agent

Because the occurrence of distributed cracks takes a lot of time and special conditions to develop, the use of expansion agent, also known

\*1 PhD. Candidate, Dept. of Civil Engineering, Tokyo Institute of Technology, JCI member.

\*2 Assistant Professor, Dr. Eng., Dept. of Civil Engineering, Tokyo Institute of Technology, JCI member.

\*3 Professor, Dr. Eng., Dept. of Civil Engineering, Tokyo Institute of Technology, JCI member.

Table 1 Mix proportions for each of the concrete batches

Concrete Type	W <sup>*1</sup> [kg/m <sup>3</sup> ]	C <sup>*2</sup> [kg/m <sup>3</sup> ]	W/C [%]	S <sup>*3</sup> [kg/m <sup>3</sup> ]	G <sup>*4</sup> [kg/m <sup>3</sup> ]	EA <sup>*5</sup> [kg/m <sup>3</sup> ]	F <sup>*6</sup> [kg/m <sup>3</sup> ]	AE <sup>*7</sup> [kg/m <sup>3</sup> ]	SP <sup>*8</sup> [kg/m <sup>3</sup> ]
C	175	350	50	788	963	-	-	2.8	1.75
00F130EA	175	350	50	678	963	130	-	2.8	1.75
00F135EA	175	350	50	674	963	135	-	2.8	1.75
05F140EA	175	350	50	670	963	140	40	2.8	2.6
10F145EA	175	350	50	666	963	145	80	2.8	2.6

\*1 Water, \*2 High early strength Portland Cement, specific gravity = 3.14, \*3 Fine aggregate, specific gravity = 2.64, \*4 Coarse aggregate, specific gravity = 2.64,  $G_{\max} = 20$  mm, \*5 Expansion agent, specific gravity = 3.14, \*6 Steel fibers, specific gravity = 7.85, \*7 Air entraining agent, type 775S, specific gravity = 1.025, \*8 Superplasticizer, high performance water reducing agent, type SP8N, specific gravity = 1.05

as shrinkage reducing admixture, came as a solution to solve this inconvenience. The amount of expansion agent was to replace a part of the fine aggregate mass and not of the cement mass. The reason behind this choice has been explained in the previous research [2].

### 3. TEST PROGRAM

The test specimens consisted in a total number of five beams, one for each of the mix proportions shown in Table 1. The beam dimensions and the reinforcement layout are shown in Fig. 1. For all the beams used in this study, a constant shear span to effective depth ratio  $a/d = 2.71$  was chosen. The goal was to obtain diagonal tension failure of the beam,  $a/d > 2.5$ , and at the same time to keep it similar to the value used previously [2] as the present study is a continuation of the earlier research work. Moreover, the longitudinal reinforcement ratio  $p_w$  is 3.28%. This high value was chosen to ensure that the beams will fail in shear and not in flexure.

As reported earlier in Toma et al. [2], the use of expansion agent created some sort of prestressing force in the RC beam, phenomenon which was termed as “chemical prestress”. In order to avoid this phenomenon, a symmetrically reinforced cross-section was used as shown in Fig.

1. In this way, the strains created due to the use of expansion agent are more uniformly distributed and, as a consequence, the values for  $\beta_n$  are expected to decrease.

After casting, the formworks were covered in wet cloth and kept at room temperature for 24 hours. The second day, the specimens were taken out from the formwork and for the next six days, they were kept at 21°C constant temperature and 75% relative humidity. The strain induced in the beams was measured with the help of strain gages attached to the longitudinal reinforcement and recorded by a data logger at 5 minutes interval. At 7 days the beams were tested for shear. The results obtained from testing as well as the strain history during the curing period of time are presented further on.

### 4. RESULTS AND DISCUSSIONS

#### 4.1 Concrete strength

Following the procedures for testing for the compressive strength and for the tensile strength according to JIS A 1108 and JIS A 1113, respectively, the measured values were  $f'_c = 31.5$  N/mm<sup>2</sup> and  $f_t = 2.2$  N/mm<sup>2</sup>, respectively. For the other cylinders obtained from the mix proportions containing the expansion agent the tests could not be performed. The concrete in the cylinders made

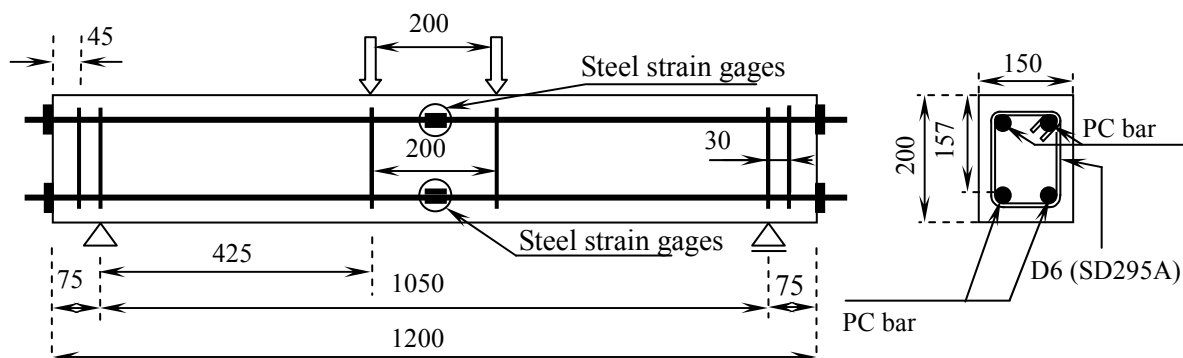


Fig.1 Beam sizes and reinforcement layout (unit: mm)

from these mix proportions, where expansion agent was used, were very weak and tended to break when lifted from the ground. An example of such a cylinder is shown in Fig. 2. However, the strength of concrete in the RC beams seems to differ from that in the cylinders since none of the beams exhibited such advanced damage.

Because of this, a non-destructive Schmidt hammer test was conducted on the concrete from the RC beams in order to evaluate its compressive strength. The number of the measured values for the Schmidt hammer test was 50 and the location of the measuring points was along the beam length and between the lines marking the location of the top and bottom longitudinal reinforcement. A more detailed explanation of the measuring procedure is given in Toma et al [2]. The results are summarized in Table 2.

By taking a look at Table 2, some interesting observations can be made. First of all, by comparing the concrete strength obtained from the Schmidt hammer test on the beams, for the control case “C”, with the value obtained from uniaxial compression test, an increase in the value for the compressive strength can be observed. This increase is due to the confining effect of the reinforcement. On the other hand, the compressive strengths for the other cases exhibit an opposite trend compared to the amount of expansion agent used in the mix proportion: the increase in the amount of expansion agent results in a decrease of

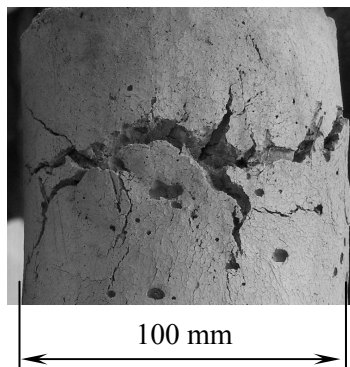


Fig.2 Cracked cylinder of the 05F140EA concrete mix

Table 2 Concrete strength in the RC beams given by the Schmidt hammer test

Concrete Type	$f'_{c, Sch}$ [N/mm <sup>2</sup> ]
C	32.8
00F130EA	20.4
00F135EA	18.7
05F140EA	16.5
10F145EA	20.4

compressive strength of the concrete from the RC beams, measured by the Schmidt hammer test. However, if the fiber percentage is increased from 0.5% to 1.0%, an increase in the compressive strength is obtained even though the amount of expansion agent is increasing. This could be explained by the fact that a higher fiber percentage is able to better confine the concrete, in addition to the confinement effect of the longitudinal reinforcement, subjected to expansion stresses.

#### 4.2 Strain history of steel

The steel strain history was monitored with the help of steel strain gages attached on both the upper and the lower side of the longitudinal reinforcement, on all four bars, at mid-span, as shown in Fig. 1. The results were recorded by a data logger on a five minutes interval. The obtained data is graphically represented in Fig. 3. The positive values of the steel strains mean that the reinforcement is in tension. The plotted values represent the average steel strains for the reinforcement located both at the bottom and at the top part of the beam, as it can be seen from Fig. 1. In some cases, e.g. “00F130EA” shown in Fig. 3, the average tensile strain in the longitudinal reinforcement at the top part is smaller than the average tensile strain in the longitudinal reinforcement at the bottom part meaning that the beam has the tendency to bend downwards. In other cases, the tendency is reversed with the beam bending upwards due to the average tensile steel strain at the top part being greater than at the bottom part.

The JSCE standard specifications for concrete structures [3] show that the value of the  $\beta_n$  factor depends both on the decompression moment  $M_0$  and on the ultimate resisting moment of the beam,  $M_u$ . Taking into account the reinforcement layout in Fig. 1, the values of  $M_u$  are higher than in the previous studies by Toma et al. [2]. For higher values of  $M_u$  smaller values of  $\beta_n$  are obtained. On the other hand, the values of  $M_0$  depend on the steel strain  $\varepsilon_s$  as shown in the study performed by Toma et al. [4]. In the present

Table 3 Influence of the chemical prestressing taken into account through the factor  $\beta_n$

Concrete Type	$\beta_n$
C	1
00F130EA	0.95
00F135EA	0.96
05F140EA	1.04
10F145EA	1.11

research, the steel strain  $\varepsilon_s$  is computed as the difference between the steel strain at the top part and the steel strain at the bottom part, Eq. 1.

$$\varepsilon_s = \varepsilon_s^{top} - \varepsilon_s^{bottom} \quad (1)$$

The smaller the values of  $\varepsilon_s$  are the smaller the values of  $M_0$  and, consequently smaller values of  $\beta_n$  are obtained. The calculated results for  $\beta_n$  are summarized in Table 3 and compared with earlier research [2]. They are indeed smaller and closer to 1.0 meaning that the used reinforcement layout is able to distribute the strains more evenly throughout the cross section of the beam. Values of  $\beta_n < 1.0$  signify that the beam bends downwards ( $M_0 < 0$  because  $\varepsilon_s^{top} < \varepsilon_s^{bottom}$ ) and values of  $\beta_n > 1.0$  mean that the beam bends upwards ( $M_0 > 0$  because  $\varepsilon_s^{top} > \varepsilon_s^{bottom}$ ).

### 4.3 Crack density

For the purpose of this research, the crack density is defined as the ratio between the area of the cracks and the uncracked area on concrete, as shown in Eq. 2:

$$\Omega_j = \frac{\bar{w}_j \cdot \sum_{i=1}^n L_i}{A_j} \quad (2)$$

in which  $\bar{w}_j$  is the average crack width, in mm, for the considered area  $A_j$ ,  $\sum_{i=1}^n L_i$  is the total crack length for the considered area  $A_j$  and  $A_j$  is the initial area of concrete under consideration. Using this method, the concrete area of a beam can be divided into any number of smaller areas followed by the calculation of the crack density for each

individual area. The beauty and the easiness of this method consists in the fact that it relies on the average crack width and on the total crack length for a specified area of concrete and not with each crack individually and thus avoiding the debate on how one defines a crack. The value of the total crack length is obtained from specialized software after manually tracing, as accurately as possible, every visible crack.

In the present study two distinct concrete area divisions have been used: first division took into consideration the concrete areas covered by the shear spans. The two areas had the dimensions on 425 mm x 200 mm (L x H) and were denoted by  $A_1$  and  $A_2$ . For this type of division 180 values were measured for the crack widths. The corresponding crack densities were computed and are shown in Fig. 4 as  $\Omega_1$  and  $\Omega_2$  for the respective areas of concrete. The values of the crack densities are shown as a percentage of the initial area of concrete for an easier understanding. Additionally, Fig. 4 shows the distributed crack patterns for all the specimens exhibiting such cracks. Please keep in mind that these cracks were obtained before the loading tests and are solely the result of using

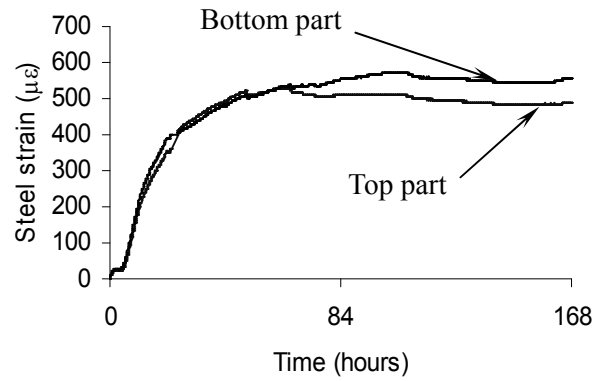


Fig. 3 Steel strain history

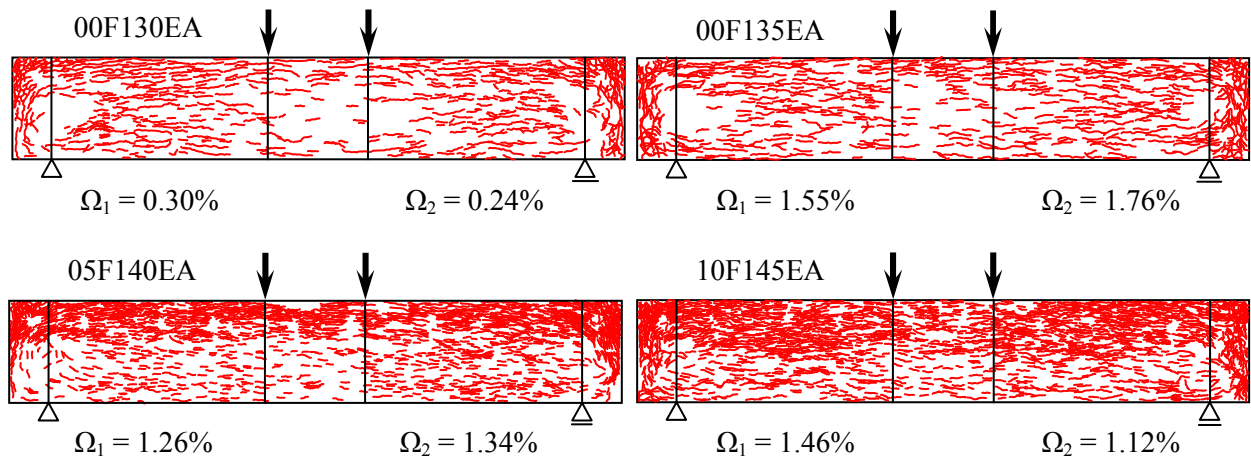


Fig. 4 Distributed crack patterns

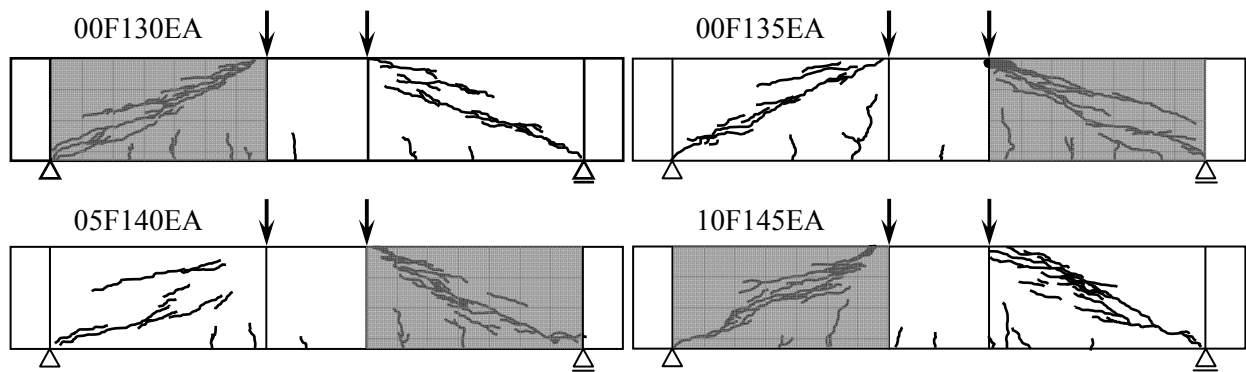


Fig. 5 Shear crack patterns for the specimens that showed distributed cracks before loading

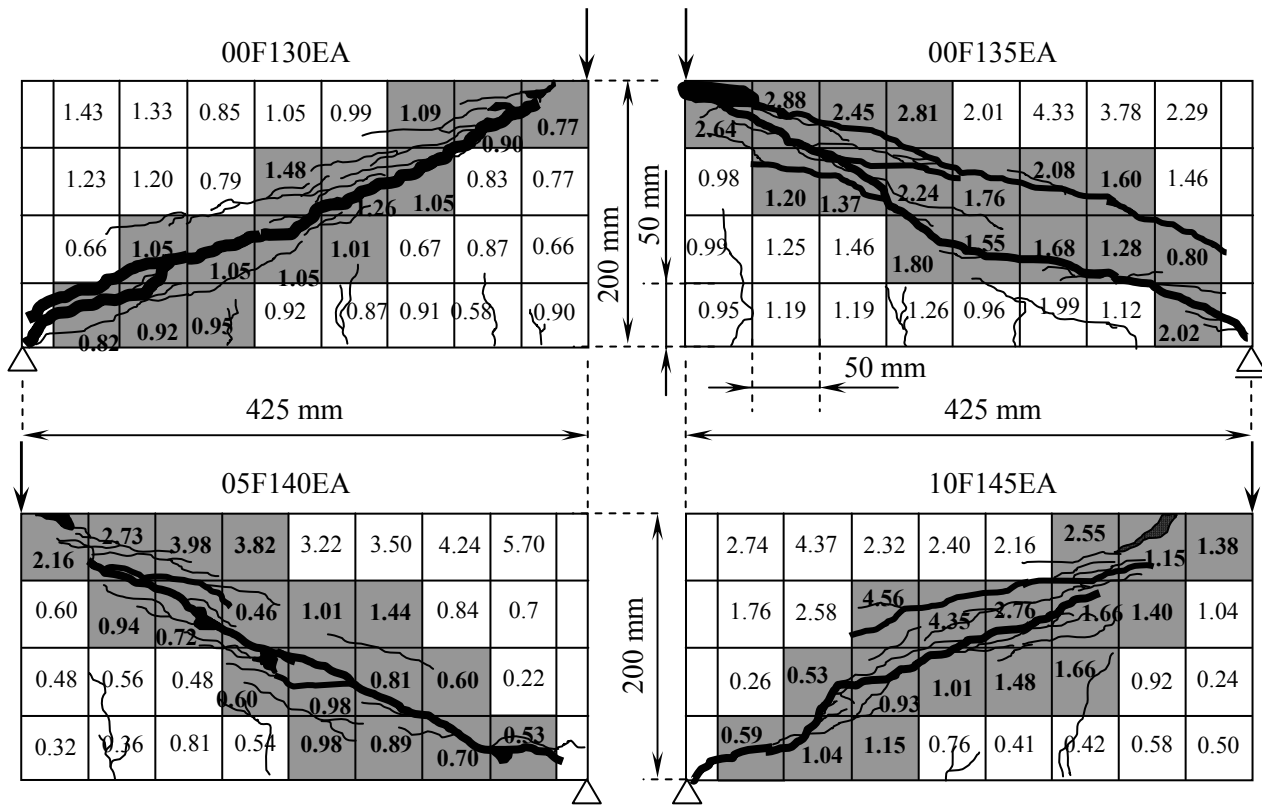


Fig. 6 Prediction of the shear crack location using the crack density parameter  $\Omega$  (%)

expansion agent.

The second type of area division was performed on the entire surface of the beam. A grid with the constant size of 50 mm in both directions was drawn on the surface of the beam. For each individual area 5 values of the crack widths were measured. Applying Eq. 2, the crack density for each of the 50 mm x 50 mm square areas was calculated. Since this paper deals with the shear failure of RC beams, the focus was only on the small areas located within the shear spans.

#### 4.4 Shear testing and shear crack location

The RC beams were subjected to a

two-point loading test until shear failure occurred. The shear crack patterns for the specimens that exhibited distributed cracks before loading, that is all the specimens except the control case, are shown in Fig. 5. The highlighted area shows the shear span where the shear failure occurred.

Taking into account also Fig. 4, an interesting observation can be made with respect to the values of  $\Omega_1$ ,  $\Omega_2$  and the location of the critical shear crack in terms of the shear span: the critical shear crack, that is the crack that was formed at the peak load and led to the failure of the specimen, is located in the shear span for which the value of the crack density parameter is

higher. This means that the crack density parameter can predict the shear span in which the shear failure is more likely to occur.

Can it predict the location of the shear crack in more detail? In order to answer this question we have to take into account the second type of area division that was previously mentioned. The procedure is similar to that used to determine in which span the failure will occur: once the location of the shear crack was found out, in terms of the shear span, the crack density for each of the 50mm x 50mm squares located in the respective shear span was computed. The obtained results are shown in Fig. 6.

The locations of the shear cracks within the shear spans where the failure will occur are depicted in shaded squares. The selection of the shaded squares is based on the values of the crack density parameter, expressed as a percentage of the initial area of concrete. High values of the crack density parameter indicate that the critical shear crack is more likely to pass through the respective squares. Moreover, it is well known that the shear stresses transfer from the loading point to the support so the focus is also on the line connecting the two points. On the other hand, the squares at the top part of each of the shown beams in Fig. 6 that are closer to the vertical line passing through the support point exhibit also quite high values of the crack density parameter. Since this area plays little role in the shear carrying capacity, the respective squares are not taken into account, despite the high values for the crack density parameter.

Based on the above mentioned assumptions, the focus is on the squares that exhibit high values of the crack density parameter and are closely located to the line joining the loading point to the support.

As it can be seen from Fig. 6, the crack density parameter can predict quite accurately the location of the shear crack in RC beams affected by distributed cracks. However, there are instances, for example 05F140EA and 10F145EA cases, when the location on the shear crack can be predicted to lie within a wider area. Instead it passes through fewer shaded squares than initially assumed. Of course, this depends on the surface area division and on the level of accuracy required for each case. If one is interested in finding only the shear span where the failure will occur, the surface area division shown in Fig. 4 is enough. However, if a more accurate prediction is required in terms of the shear crack location within the shear span, other area divisions should be taken into account, for example as shown in Fig. 6.

## 5. CONCLUSIONS

- 1) A new procedure to mathematically quantify the effect of distributed cracks on RC beams has been proposed through the crack density parameter. The method is quite straight forward and easy to use because it deals with the average width of the cracks within a certain area of concrete and with the total crack length within that area and thus avoiding the debate of how one defines a crack.
- 2) The crack density parameter proved to be a very useful tool in predicting the location of the shear crack for RC beams affected by distributed cracks. The prediction can range from the shear span where the failure is more likely to occur and can be extended to give almost the exact location of the shear crack within the shear span.
- 3) Even though the proposed method showed promising results there were cases when the predicted areas within which the shear crack would be located were slightly wider than the ones obtained from the overlapping of the experimental results. Further tests should be conducted in order to clarify whether the overestimation was due to the way of the division of the surface area or due to the number of measured crack width values for each area.

## REFERENCES

- [1] W. J. Kreffeld and C. W. Thurston: Studies on the Shear and Diagonal Tension Strength of Simply Supported Reinforced Concrete Beams, *ACI Journal*, 63(4), pp. 451-476, 1966
- [2] I.O. Toma, T. Miki and J. Niwa: Influence of random cracks on the shear behavior of reinforced concrete beams containing steel fibers, *Doboku Gakkai Ronbunshuu E*, Vol. 63, No. 1, pp. 66-78, 2007
- [3] JSCE: Standard Specifications for Concrete Structures – Structural Performance Verification, *JSCE Guidelines for Concrete* No. 3, pp. 76, 2002
- [4] I. O. Toma, T. Miki and J. Niwa: Influence of Steel Fibers on the Behavior of RC Beams with Random Cracks, *The 10<sup>th</sup> East Asia-Pacific Conference on Structural Engineering and Construction (EASEC - 10)*, Materials, Experimentation, Maintenance and Rehabilitation, Bangkok, Thailand, pp. 413-418, Aug. 2006